

Somatic *STAT3* mutations in Felty syndrome: an implication for a common pathogenesis with large granular lymphocyte leukemia

Paula Savola,^{1,2} Oscar Brück,^{1,2} Thomas Olson,³ Tiina Kelkka,^{1,2}
Markku J. Kauppi,^{4,5} Panu E. Kovanen,⁶ Soili Kytölä,⁷ Tuulikki Sokka-Isler,⁸ Thomas P. Loughran,³
Marjatta Leirisalo-Repo⁹ and Satu Mustjoki^{1,2}

¹Hematology Research Unit Helsinki, University of Helsinki and Department of Hematology, Helsinki University Hospital Comprehensive Cancer Center, Finland; ²Department of Clinical Chemistry and Hematology, University of Helsinki, Finland; ³University of Virginia Cancer Center; University of Virginia, Charlottesville, VA, USA; ⁴Päijät-Häme Central Hospital, Lahti, Finland; ⁵Faculty of Medicine, Tampere University, Finland; ⁶Department of Pathology, University of Helsinki and HUSLAB, Helsinki University Hospital, Finland; ⁷Laboratory of Genetics, HUSLAB, Helsinki University Hospital, Finland; ⁸Rheumatology/Medicine, Jyväskylä Central Hospital, Finland and ⁹Rheumatology, University of Helsinki and Helsinki University Hospital, Finland

©2017 Ferrata Storti Foundation. This is an open-access paper. doi:10.3324/haematol.2017.175729

Received: July 13, 2017.

Accepted: December 6, 2017.

Pre-published: December 7, 2017.

Correspondence: satu.mustjoki@helsinki.fi

Supplementary Material

Somatic *STAT3* mutations in the Felty syndrome: an implication for a common pathogenesis with LGL leukemia

Paula Savola^{1,2}, Oscar Brück¹, Thomas Olson³, Tiina Kelkka^{1,2}, Markku J. Kauppi^{4,5}, Panu E. Kovanen⁶, Soili Kytölä⁷, Tuulikki Sokka-Isler⁸, Thomas P. Loughran³, Marjatta Leirisalo-Repo⁹, and Satu Mustjoki^{1,2}

¹Hematology Research Unit Helsinki, University of Helsinki and Department of Hematology, Helsinki University Hospital Comprehensive Cancer Center, Helsinki, Finland

²Department of Clinical Chemistry and Hematology, University of Helsinki, Helsinki, Finland

³University of Virginia Cancer Center; University of Virginia, Charlottesville, Virginia, USA

⁴Päijät-Häme Central Hospital, Lahti, Finland

⁵Faculty of Medicine, Tampere University, Tampere, Finland

⁶Department of Pathology, HUSLAB and Haartman Institute, University of Helsinki and Helsinki University Hospital, Helsinki, Finland

⁷Laboratory of Genetics, HUSLAB, Helsinki University Hospital, Helsinki, Finland

⁸Rheumatology/Medicine, Jyväskylä Central Hospital, Jyväskylä, Finland

⁹Rheumatology, University of Helsinki and Helsinki University Hospital, Helsinki, Finland

Supplemental methods

Patient recruitment

The diagnosis of FS is defined by RA, neutropenia, and splenomegaly. We included patients with an established Felty syndrome diagnosis (n=14) that was stated in patient records. Patients were identified by querying the hospital electronic patient record system for the ICD-10 code M5.0 and by inquiring treating rheumatologists for FS patients. Clinical information was retrospectively gathered from patient records. The ethical boards of our institutions approved this study, and the declaration of Helsinki guidelines were followed. Patients gave written informed consent.

Sample preparation

DNA samples from different cell types were obtained (Supplementary Table 1 and Supplementary Figure 1). For six patients, only archived samples were available. Eight patients gave new blood samples for the study. Mononuclear cells were obtained from EDTA whole blood via Ficoll gradient centrifugation (Ficoll-Paque PLUS, GE Healthcare). CD8⁺ cells were obtained with magnetic bead (Miltenyi Biotech) positive selection from mononuclear cells. Purity of sorted cells was confirmed with flow cytometry with the FACSVerse or FACS Aria II instrument (Beckton Dickinson). Data was analyzed with FlowJo software.

Flow cytometry was used to screen the blood samples for large T-cell clones: a panel of antibodies against the different variable beta regions of the T-cell receptor (IO Test V β mark kit, Beckman Coulter), accompanied by anti-CD3 (SK7), anti-CD4 (SK3), and anti-CD8 (SK-1) (Becton Dickinson) antibodies was used. The V β kit covers approximately 70% of the V β T-cell repertoire. Sorting of expanded CD8⁺ T-cell populations expressing a specific V β was performed on the FACS Aria II instrument, and purities of

sorted cells was controlled by flow cytometry. Cells were stained with the same antibodies as in the V β analysis.

DNA was extracted according to manufacturer's instructions using DNA Tissue kit (Machery Nagel). For some patients, bone-marrow mononuclear-cell DNA and/or whole-blood DNA, originally obtained for clinical TCR γ gene rearrangement testing for clinical purposes, were available. Also, methanol-fixed cells, originally obtained for chromosome analysis were available from some patients (Supplementary Table 1). From these methanol-fixed cells, methanol was washed with a dilution series followed by DNA extraction with the DNA Tissue kit (Machery Nagel).

***STAT3* and *STAT5B* sequencing**

Amplicon sequencing of 23 exons of the *STAT3* gene and *STAT5B* exon 16 was performed from the DNA samples. Amplicon sequencing is a PCR-based next-generation sequencing method that enables very high sequencing depths (up to over 100,000x). Thus, it detects variants with a very low variant-allele frequency (VAF), locally reaching the sensitivity of 0.5%.¹

A 2-step PCR was performed for the DNA samples. The first PCR was performed in 20 μ l containing 10ng of DNA, 10 μ l of 2 \times Phusion High-Fidelity PCR Master Mix and 0.375 μ M of each locus-specific primer, adjusted to the final volume with water. The second PCR was performed in 20 μ l containing 1 μ l of the amplified product from the first PCR, 10 μ l of 2 \times Phusion High-Fidelity PCR Master Mix, 0.375 μ M of index primer 1 and 0.375 μ M of index primer 2.

The first PCR reaction was cycled with DNA Engine Tetrad 2 (Bio-Rad Laboratories) or G-Storm GS4 (Somerton) according to the program: 98°C 30s, 30 cycles at 98°C for 10s, at 59-63°C for 30s, and at 72°C for 15s, and final extension at 72°C for 10 minutes. The second PCR was cycled with the following program: initial denaturation at 98°C 30s, 8 cycles at 98°C for 10s, at 65°C for 30s, and at 72°C for 20s, and the final extension at 72°C for 5 minutes.

The amplified samples were pooled without exact quantification and Agencourt AMPure XP beads (Beckman Coulter) were used twice using 0.8x volume of beads to purify the amplified sample pools. This removes primer dimers. Sample pools were quantified using Agilent 2100 Bioanalyzer (Agilent Genomics). Sequencing was performed using the Illumina MiSeq System.

Sequencing reads were aligned to the human hg19 genome with Bowtie2, and GATK IndelRealigner was used for local realignment near indels. Reads with low quality were not excluded, but were aligned to the genome. In further analyses, quality scores were used to exclude error bases. Variants with over 5 counts and VAF over 0.5% were called. A specific frequency ratio was calculated by dividing the ratio of variant calls/number of all the bases (at a position) by the ratio of variant allele quality sum/quality sum of all bases. False positive variants were filtered out using this ratio: variants with a frequency ratio <0.8 were excluded. In this study, we considered the mutation to be true if occurred in the sequenced sample with a VAF >1% and absent in control samples. All primers are listed in Supplementary Table 2.

Cytokine profiling

We performed cytokine profiling to study the possible differences between RA, FS, and LGL leukemia. EDTA plasma samples from 8 healthy controls, 9 RA patients, 7 FS patients, and 9 LGL leukemia patients were used for the assay. All subjects had given written informed consent. Cytokines were analyzed with Proseek Multiplex Inflammation I (Olink Biosciences) immunoassay that detects 92 different biomarkers simultaneously in one sample.

The assay utilizes proximity extension assay technology, in which oligonucleotide-labeled antibodies bind their targets, and the target-antibody complexes are detected with real-time PCR. After overnight incubation with Olink's incubation mix (1µl plasma sample), the extension reaction was performed by incubating the reagents for 5 minutes at room temperature with the PEA enzyme, and PCR was performed using PCR polymerase and 96.96 dynamic array Biomark HD (Fluidigm) machine. A list of the analyzed biomarkers is presented in Supplementary Table 3.

The assay does not allow reporting protein concentrations, but values are reported as normalized protein expression units (NPX). NPX-values are obtained from Cq values after normalizing against the extension control, interplate control and correction factor, and are reported in log2 scale.

1. $dCq_{analyte} = Cq_{analyte} - Cq_{Ext Ctrl}$
2. $ddCq_{analyte} = dCq_{analyte} - dCq_{Interplate Ctrl}$
3. $NPX = Correction\ factor - ddCq_{analyte}$

NPX values from the same cytokine are comparable between patients, but the values of different cytokines cannot be directly compared. Data analysis was performed with NPX

values with Qlucore Omics Explorer (Qlucore). Qlucore Omics Explorer uses the Benjamini-Hochberg method to calculate q-values (false discovery rates) from the p-values. Cytokines with a false discovery rate <0.1 were reported and further post-hoc testing was performed using Dunn's multiple comparison tests.

Immunohistochemistry

To study phosphorylation of STAT3, we stained bone-marrow biopsy samples from 7 patients. The bone-marrow biopsies had been obtained previously to examine possible reasons for neutropenia, and the remaining material had been archived. We recruited control subjects with a bone marrow biopsy taken in 2010 in the Helsinki University Central Hospital (HUCH) for clinical purposes. The controls did not have cancer nor immunologic disease in six years of follow-up (n=14). A tissue microarray (TMA) was constructed from duplicate 1 mm punches.

According to standard clinical procedure, fresh bone marrow biopsies were formalin-fixed and paraffin-embedded (FFPE) in the Department of Pathology, HUCH. FFPE tissue blocks were cut in 3.5 µm sections on Superfrost objective slides (Kindler O GmbH, Germany) with the Microm 355S microtome (Thermo Scientific, Waltham, MA). Glass slides were dried overnight at +37°C and stored for short-term use at +4°C. All consecutive phases were performed in room temperature unless otherwise specified. Protein blocking and antibody incubations were performed in a humid chamber. Slides were washed three times with 0.1% Tween-20 (Thermo Fisher Scientific) diluted in 10 mM Tris-HCL buffered saline pH 7.4 (TBS) after peroxide block, antibody incubations, and fluorochrome reaction.

Slides were deparaffinized in xylene and rehydrated in graded ethanol series and H₂O. Heat-induced epitope retrieval (HIER) was carried out in 10 mM Tris-HCl - 1 mM EDTA buffer (pH 9) in +99°C for 20 min (PT Module, Thermo Fisher Scientific, Waltham, MA). Peroxide activity was blocked in 0.9% H₂O₂ solution for 15 min, and subsequently 10% normal goat serum (TBS-NGS) applied for 15 min.

CD57 (clone VC1.1, Sigma-Aldrich) and pSTAT3 (Tyr705, Cell Signaling) diluted 1:100 and 1:250, respectively, in protein block solution were applied for 1h30min.

Horseradish peroxidase (HRP)-conjugated anti-mouse and alkaline phosphatase (AP)-conjugated anti-rabbit secondary antibodies (Immunologic) mixed 1:1 were applied for 45 min. To detect antibody complexes red (Liquid Permanent Red; Dako) and green (VinaGreen; Biocare Medical, Concord, CA) chromogens were used according to manufacturer's instructions. Slides were counterstained using Mayer's hematoxylin diluted 1:10 in H₂O for 1min30s. Slides were washed in H₂O for 30 s after each chromogen reaction. Finally, slides were mounted with Pertex and coverslips.

Tissues were digitalized at 0.33 μ m/pixel resolution using Pannoramic P250 Flash II tissue slide scanner (3DHistech, Hungary) with Zeiss Plan-Apochromat 20x objective (NA 0.8).

Statistics

Multiplex cytokine data was analyzed with NPX values with Qlucore Omics Explorer (Qlucore). Cytokines with a false discovery rate <0.1 (Benjamini-Hochberg method) were reported and further post-hoc testing was performed using Dunn's multiple comparison tests. Statistical analyses for the clinical data were performed with

GraphPad Prism software. Statistical tests included Kruskal-Wallis omnibus test, Dunn's multiple comparison test, Mann-Whitney test and Fisher's exact test.

Supplementary Table 1. All sample types collected and *STAT3* mutations in the samples.

	BM MNC	BM cells	PWB	PB MNC	PB CD8+	PB CD8 ^{neg}	PB CD4+
1	X, 2.9%	X, 8.9%					
2	X, 2.0%		X		X	X	
3	X	X	X		X, 1%	X	
4			X, 1.4%		X, 8.8%		X
5		X, 1.6%/1.1%	X, 2.4%/3.0%				
6	X, 5.7%	X, 3.3%			X, 1.4%		X
7				X			
8				X			
9	X	X	X				
10				X			
11				X			
12				X			
13					X		X
14					X		X
Total	5	5	5	5	6	2	3
Mutations	3	4	3	0	3	0	0

Time of sample obtaining:

	First sample
	0-1 years after obtaining first sample
	Over 1 year after obtaining first sample (range 2-12)

For many patients, several types of samples were available. Each patient is shown on one row, and columns have X if the applicable sample type was available from the patient. If a *STAT3* mutation was detected in the sample, the variant allele frequency is presented after the X. Patient 5 had two different *STAT3* mutations (N647I and Y640F), and the variant allele frequencies of both mutations are presented. Abbreviations: BM MNC, bone-marrow mononuclear-cell DNA; BM cells, cultured-cell DNA from the bone marrow (cells originally obtained for chromosome analysis); PWB peripheral whole-blood DNA; PB MNC, peripheral-blood mononuclear-cell DNA; PB CD8+, peripheral-blood CD8+ cell-DNA; PB CD8^{neg}, peripheral-blood CD8-negative-cell DNA; PB CD4+, Peripheral-blood CD4+ cell-DNA.

Supplementary Table 2. *STAT3* and *STAT5B* amplicon sequencing primers.

#	Primer name	Primer sequence
1	STAT3_2-F	TCCCCATCACCTGTACCCAT
2	STAT3_2-R	TGACACCTGTGTTGGGCAAT
3	STAT3_3-F	ACACTAACACCCGACTCTGC
4	STAT3_3-R	TGTATGCGTCGGCTTCAGAG
5	STAT3_4-F	TCCATTCCCTCCAGACCAGG
6	STAT3_4-R	GCTCTGAAGCCTTTGTTCCG
7	STAT3_5-F	CCGAGGCTTGTAACCTGTCAT
8	STAT3_5-R	TTCCCTTCCTCTTGTGATGG
9	STAT3_6-F	GACCAGGCTCCTTTGAGGAC
10	STAT3_6-R	CTCTTGGGGATACTGCCTGC
11	STAT3_7-F	CCGATCTAGGCAGATGTTGG
12	STAT3_7-R	TTCCCTCAGGTCAAGGAGTTT
13	STAT3_8-F	CTGTGGGCCTGCAGTTAAGA
14	STAT3_8-R	GTTCCCTGCTCTGGAGTTGACT
15	STAT3_9-F	AAGAGAAGATGGGCTCACGC
16	STAT3_9-R	TCCCCTTCTCCATCTCACCT
17	STAT3_10-F	TGGAAAGAATGACCCTGGCC
18	STAT3_10-R	CACGTGGTAGAGTGAGAGGC
19	STAT3_11-F	AATGCACCCCAAGGCTTTTG
20	STAT3_11-R	CCTCCACAGTGCTGAGATT
21	STAT3_12-14-F	CAAGGAAAACACCCCAGTTG
22	STAT3_12-14-R	AAATAACAGGTGGTCAAAGTAGGC
23	STAT3_15-F	ATTGCCAGATGGGATGCCAA
24	STAT3_15-R	CCACACCTGGCCTAAGAGTG
25	STAT3_16-F	GAGGAGAAGTCCAGCTCAG
26	STAT3_16-R	CCTTTCATTCTGAGCCCCGT
27	STAT3_17-F	AGGGAGAAGGGGTGAAATGC
28	STAT3_17-R	TGCCCCCTCCTTTTAGTTGG
29	STAT3_18-F	CCTTGCCAGCCATGTTTTCC
30	STAT3_18-R	AACCTCTTGACCCCAAGCTG
31	STAT3_19-F	GTGCACACTCTGTCCAACCT
32	STAT3_19-R	GCTTGAAGGCCCTGAACTCT
33	STAT3_20-F	GGAGTCAAGGCCATCTCCAC
34	STAT3_20-R	TGGATGCCCTGTTAGCAATA
35	STAT3_21-F	CCAAAAATTAAATGCCAGGA
36	STAT3_21-R	GGTTCATGATCTTTCCTTCC
37	STAT3_22-F	CTCACCCAGTGTCCTTCC
38	STAT3_22-R	GGCAGATGGAGCTTCCAGA
39	STAT3_23-F	GACCAGCTCTCGGTGTGTAC
40	STAT3_23-R	TGGAGACCAGAGTTTGATGGC
41	STAT3_24-F	GGCACTTGCTAAGAACAACA
42	STAT3_24-R	AGTTGCAGAGGGTGGACAAC
43	STAT5B_16-F	TGTTGGGGTTTTAAGATTCC
44	STAT5B_16-R	CAAATCAGAATGCGAACATTG
45	STAT5A_17-F	TCCTGCTGCTGGTGGATTAT
46	STAT5A_17-R	AGCCCAAGGCTTTGTCTATG

Supplementary Table 3. Biomarkers measured in patient plasma samples.

Target

Adenosine Deaminase (ADA)
Artemin (ARTN)
Axin-1 (AXIN1)
Beta-nerve growth factor (Beta-NGF)
Brain-derived neurotrophic factor (BDNF)
Caspase 8 (CASP-8)
C-C motif chemokine 4 (CCL4)
C-C motif chemokine 19 (CCL19)
C-C motif chemokine 20 (CCL20)
C-C motif chemokine 23 (CCL23)
C-C motif chemokine 25 (CCL25)
C-C motif chemokine 28 (CCL28)
CD40L receptor (CD40)
CUB domain-containing protein 1 (CDCP1)
C-X-C motif chemokine 1 (CXCL1)
C-X-C motif chemokine 5 (CXCL5)
C-X-C motif chemokine 6 (CXCL6)
C-X-C motif chemokine 9 (CXCL9)
C-X-C motif chemokine 10 (CXCL10)
C-X-C motif chemokine 11 (CXCL11)
Cystatin D (CST5)
Delta and Notch-like epidermal growth factor-related recep (DNER)
Eotaxin-1 (CCL11)
Eukaryotic translation initiation factor 4E-binding protein 1 (4E-BP1)
Fibroblast growth factor 5 (FGF-5)
Fibroblast growth factor 19 (FGF-19)
Fibroblast growth factor 21 (FGF-21)
Fibroblast growth factor 23 (FGF-23)
Fms-related tyrosine kinase 3 ligand (Flt3L)
Fractalkine (CX3CL1)
Glial cell line-derived neurotrophic factor (hGDNF)
Hepatocyte growth factor (HGF)
Interferon gamma (IFN-gamma)
Interleukin-1 alpha (IL-1 alpha)
Interleukin-2 (IL-2)
Interleukin-2 receptor subunit beta (IL-2RB)
Interleukin-4 (IL-4)
Interleukin-5 (IL-5)
Interleukin-6 (IL-6)
Interleukin-7 (IL-7)
Interleukin-8 (IL-8)
Interleukin-10 (IL-10)
Interleukin-10 receptor subunit alpha (IL-10RA)
Interleukin-10 receptor subunit beta (IL-10RB)

Interleukin-12 subunit beta (IL-12B)
Interleukin-13 (IL-13)
Interleukin-15 receptor subunit alpha (IL-15RA)
Interleukin-17A (IL-17A)
Interleukin-17C (IL-17C)
Interleukin-18 (IL-18)
Interleukin-18 receptor 1 (IL-18R1)
Interleukin-20 (IL-20)
Interleukin-20 receptor subunit alpha (IL-20RA)
Interleukin-22 receptor subunit alpha-1 (IL-22 RA1)
Interleukin-24 (IL-24)
Interleukin-33 (IL-33)
Latency-associated peptide transforming growth factor beta 1 (LAP TGF-beta-1)
Leukemia inhibitory factor (LIF)
Leukemia inhibitory factor receptor (LIF-R)
Macrophage colony-stimulating factor 1 (CSF-1)
Macrophage inflammatory protein 1-alpha (MIP-1 alpha)
Matrix metalloproteinase-1 (MMP-1)
Matrix metalloproteinase-10 (MMP-10)
Monocyte chemotactic protein 1 (MCP-1)
Monocyte chemotactic protein 2 (MCP-2)
Monocyte chemotactic protein 3 (MCP-3)
Monocyte chemotactic protein 4 (MCP-4)
Natural killer cell receptor 2B4 (CD244)
Neurotrophin-3 (NT-3)
Neurturin (NRTN)
Oncostatin-M (OSM)
Osteoprotegerin (OPG)
Programmed cell death 1 ligand 1 (PD-L1)
Protein S100-A12 (EN-RAGE)
Signaling lymphocytic activation molecule (SLAMF1)
SIR2-like protein 2 (SIRT2)
STAM-binding protein (STAMPB)
Stem cell factor (SCF)
Sulfotransferase 1A1 (ST1A1)
T-cell surface glycoprotein CD5 (CD5)
T cell surface glycoprotein CD6 isoform (CD6)
Thymic stromal lymphopoietin (TSLP)
TNF-beta (TNFB)
TNF-related activation-induced cytokine (TRANCE)
TNF-related apoptosis-inducing ligand (TRAIL)
Transforming growth factor alpha (TGF-alpha)
Tumor necrosis factor (Ligand) superfamily, member 12 (TWEAK)
Tumor necrosis factor (TNF)
Tumor necrosis factor ligand superfamily member 14 (TNFSF14)
Tumor necrosis factor receptor superfamily member 9 (TNFRSF9)
Urokinase-type plasminogen activator (uPA)

Supplementary Table 4. Comorbidities of the study patients.

Patient ID	Immune-mediated diseases and malignancies
1	lung epidermoid carcinoma, COPD
2	Celiac disease, cervical adenocarcinoma with single brain and liver metastasis*
3	Nodular goiter, allergies, heparin-induced thrombopenia
4	Asthma, COPD
5	Diffuse large B-cell lymphoma*
6	Celiac disease, secondary Sjögren syndrome, osteoarthritis
7	Celiac disease, immune thrombocytopenia and HLA immunization against thrombocytes, liver cirrhosis & fibrosis, hepatocellular carcinoma
8	Gout
9	Polymyalgia rheumatica, lymph-node tuberculosis
10	Possible Ig deficiency, asthma
11	no
12	no
13	bronchiectasia, osteoarthritis, celiac disease
14	no

*Patient had received chemotherapy for cervical adenocarcinoma before obtaining the *STAT3*-mutation harboring sample. However, the Felty syndrome diagnosis was established years before the cancer, and the bone marrow karyotype before and after chemotherapy was normal.

**Lymphoma was diagnosed 4 years after Felty syndrome diagnosis, and the patient's bone marrow flow cytometry analysis did not reveal abnormal B cells at the time-point from which *STAT3* sequencing was performed.

Supplementary Table 5. Medication history

Patient	Medication history	Highest MTX dose used?	Neutro/leucopenia associated with medication?	Comments
1	AuT, podophyllotoxin, SS, CyA, OXI, MTX, GC	10mg	Cytopenia continued after cessation of DMARD	
2	MTX, AuT, GC	2.5mg	Cytopenia continued after cessation of DMARD	
3	MTX, SS, OXI, GC, CyA	15mg	Cytopenia evolved without DMARD; after CyA&prednisolone initiation, neutrophils normalized.	
4	MTX, OXI, GC	7.5mg	Cytopenia evolved without DMARD; after low-dose corticosteroid and DMARD (OXI, later MTX) initiation, neutrophils normalized	
5	auranofin, SS, chloroquine, OXI, MTX, GC	15mg	Cytopenia evolved without DMARD; after MTX and prednisolone initiation, neutrophil counts increased	
6	MTX, OXI, SS, GC	15mg	Cytopenia continued after cessation of all DMARD; neutrophil count improved after re-initiation of low-dose prednisolone, OXI, and later MTX	
7	OXI, GC, AuT, MTX	5mg	Cytopenia continued after cessation of DMARD	
8	chloroquine, MTX, OXI, GC	20mg	Cytopenia before DMARD initiation; no change after DMARD usage	
9	MTX, GC	12.5mg	Cytopenia evolved without DMARD; improved after initiation of corticosteroids. MTX added on later and corticosteroids left out.	Tuberculosis medication: RMP+INH+levofloxacin, PZA
10	Leflunomide OXI	none	Cytopenia continued after cessation of DMARD	
11	Gold, etanercept, infliximab, GC, MTX	17.5mg	Cytopenia evolution unknown, neutrophil counts returned to normal with etanercept and MTX reduced to 7.5 mg.	
12	GC, etanercept, MTX	5mg	Cytopenia continued after cessation of DMARD, improvement of counts with GC.	
13	MTX, OXI, SS, GC, AuT	unknown	Cytopenia continued after cessation of DMARD	
14	MTX, SS, OXI, AZA, abatacept, GC	20mg	Cytopenia continued after cessation of DMARD	

Abbreviations: DMARD, disease-modifying anti-rheumatic drugs; LD, low-dose; MTX, methotrexate; SS, sulphasalazine; OXI, hydroxychloroquine; GC, glucocorticoids; CyA, cyclosporine A; AuT, aurothiomalate; RMP, rifampicin; INH, isoniazid; PZA, pyrazinamide.

Supplementary Table 6. Clinical characteristics of the RA patients without Felty syndrome used in the study.

Chronic RA	Sex	Serostatus	Age at dg	Disease duration at sampling (years)
palindromic RA	F	pos	43	12
palindromic RA	F	pos	51	6
palindromic RA	F	pos	64	6
palindromic RA	F	pos	55	4
palindromic RA	M	pos	60	9
palindromic RA	F	pos	56	4
palindromic RA	F	pos	27	11
palindromic RA	F	neg	61	9
RA	M	pos	72	3
RA	F	pos	44	2.5
seronegative, destructive RA	F	neg	50	17.5
seronegative, destructive RA	F	neg	16	22
seronegative, destructive RA	F	neg	28	34
seronegative, destructive RA	F	neg	28	31

Clinical characteristics of the patients with chronic RA who underwent *STAT3* exon 21 and *STAT5A/B* exon 17/16 deep sequencing. No mutations were detected. The median coverage for *STAT3* was 15737 (range 4371-33603), for *STAT5B* 16235 (range 5572-57944), and for *STAT5A* 3604 (range 855-9264). The seronegative, destructive RA patients have experienced a severe disease, and are described in more detail by a previous report.²

Supplementary Table 7. Clinical characteristics of the LGL leukemia patients screened with the cytokine panel.

Age at dg	Sex	Age at sampling	RA	Largest CD8+ clone, % of CD8+	Vβ	STAT3 mutation?	VAF	Anemia	Neutropenia	Thrombocytopenia	Leukopenia	Splenomegaly
54	M	61	no	ND	ND	no	no	yes	no	no	no	no
50	F	53	no	17%	17	no	no	no	no	yes	no	yes
53	F	54	yes	90%	8	Y640F	51%	no	yes	no	no	no
59	M	61	no	89%	3	no	no	no	no	no	no	no
57	M	59	yes	5.1%	14	Y657ins nonsense	5.9%	yes	yes	no	no	yes
58	F	65	no	76%	1	Y640F	27%	no	yes	yes	yes	no
67	F	75	no	52%	4	Y640F	25%	yes	yes	yes	yes	no
66	F	67	no	21%	14	no	no	no	yes	yes	yes	no
63	F	64	yes	2.6%*	9	D661Y	37%*	yes	yes	no	no	yes

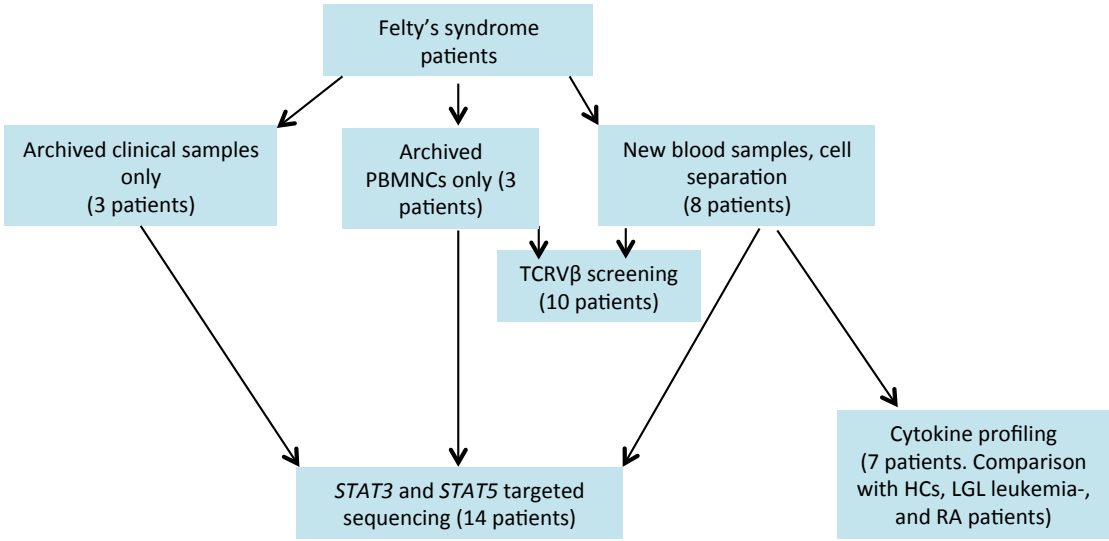
Clinical characteristics of the LGL leukemia patients that were analyzed with the cytokine panel. All cases were T-LGL leukemia. Eight of the nine patients were screened with flow cytometry for large CD8+ T-cell clones, and the clone size and the Vβ of the clone is shown. Abbreviations: dg, diagnosis; RA, rheumatoid arthritis; Vβ, Variable beta family of the largest CD8+ T cell clone analyzed by flow cytometry; VAF, variant allele frequency. *The difference in VAF and size of the largest clone by flow analysis suggests that patient had another Vβ expansion that was not detected by the flow-cytometry-based assay.

Supplementary table 8. Healthy controls and RA patients used in the cytokine panel.

	Sex	Age at sampling (years)	Disease duration at sampling (years)	Serostatus
RA	F	70	9	neg
RA	F	59	4	pos
RA	F	70	6	pos
RA	F	77	0	neg
RA	F	68	0	pos
RA	F	63	0	neg
RA	F	62	0	pos
RA	M	68	0	neg
RA	F	68	0	pos
Median		68	0	
HC	M	49	NA	NA
HC	F	43	NA	NA
HC	F	36	NA	NA
HC	F	24	NA	NA
HC	F	29	NA	NA
HC	F	59	NA	NA
HC	M	65	NA	NA
HC	F	28	NA	NA
Median		39,5		

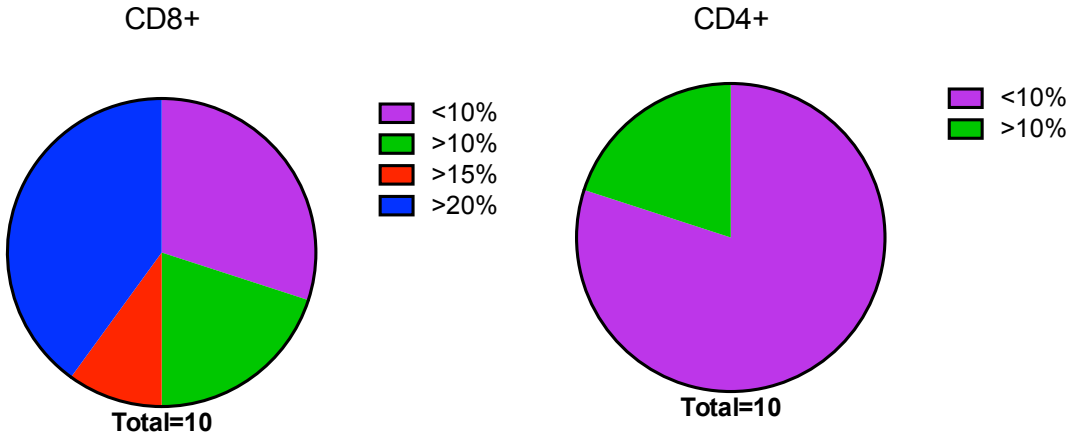
Abbreviations: F, female; M, male; NA, not applicable.

Supplementary Figure 1. Schematic of the patient sample acquisition.



FS patient samples were collected from different sources: new blood samples, frozen PBMNC samples, and archived samples that were originally acquired for clinical purposes (TCR rearrangement assays, chromosome assays). TCRV β screening results are available from only 10/11 eligible patients due to technical reasons. Abbreviations: PB, peripheral blood; MNC, mononuclear cell; HC, healthy control; RA, rheumatoid arthritis.

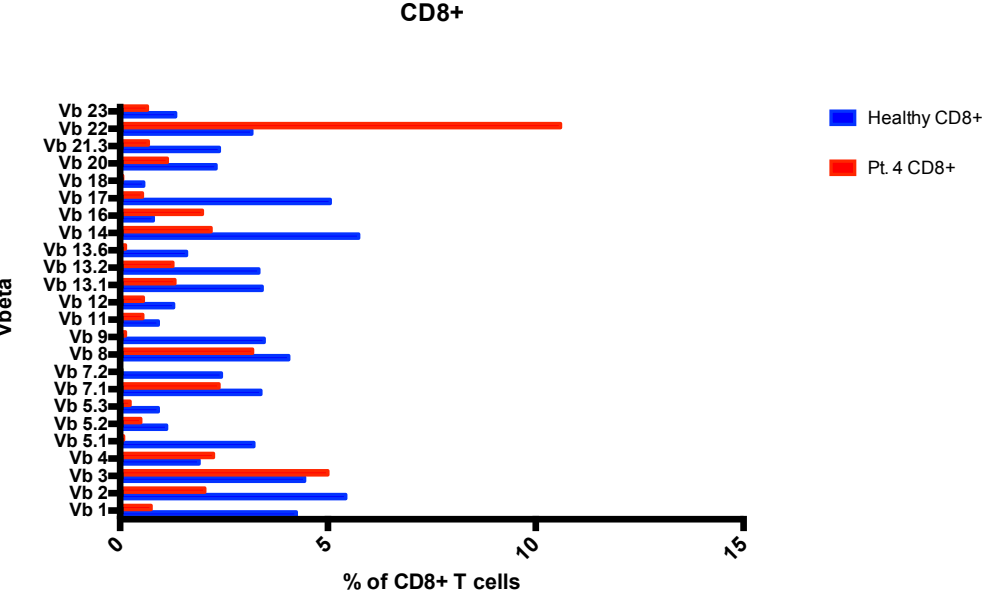
Supplementary Figure 2. Felty syndrome patients harbor large Vβ T-cell expansions.



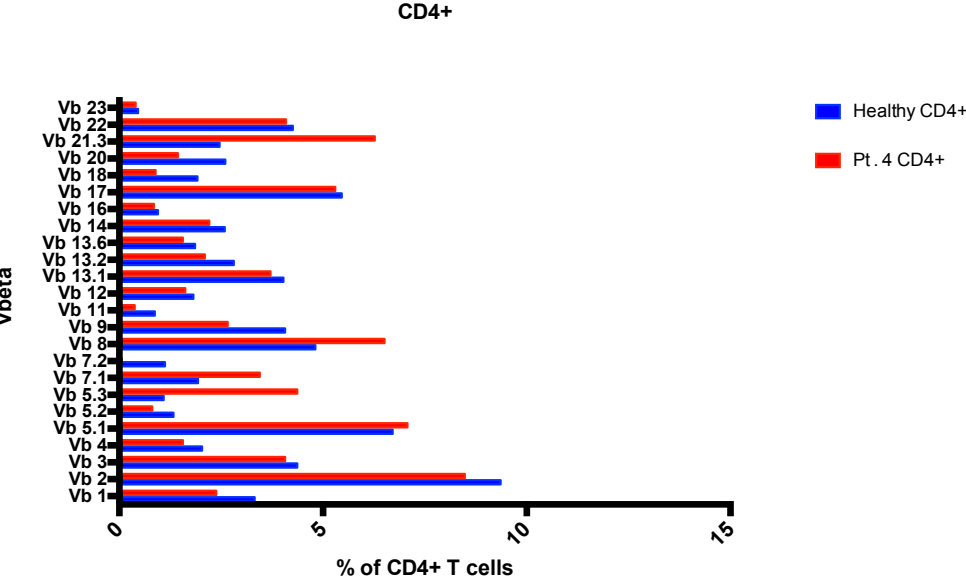
The frequency of patients harboring large CD3+CD8+ and CD3+CD4+ expansions, as detected with variable β region –specific antibodies with flow cytometry. The coloring denotes for the size of the expanded population (% of all CD8+ or CD4+ T cells). From 10 patients from whom samples were available, four patients had Vβ T-cell expansions that comprised over 20% of all CD8+ T-cells (the largest expansion 52% in patient 10) and three patients had populations >10%.

Supplementary figure 3. The CD8+ TCR repertoire of patient 4 by Vβ flow cytometry.

A

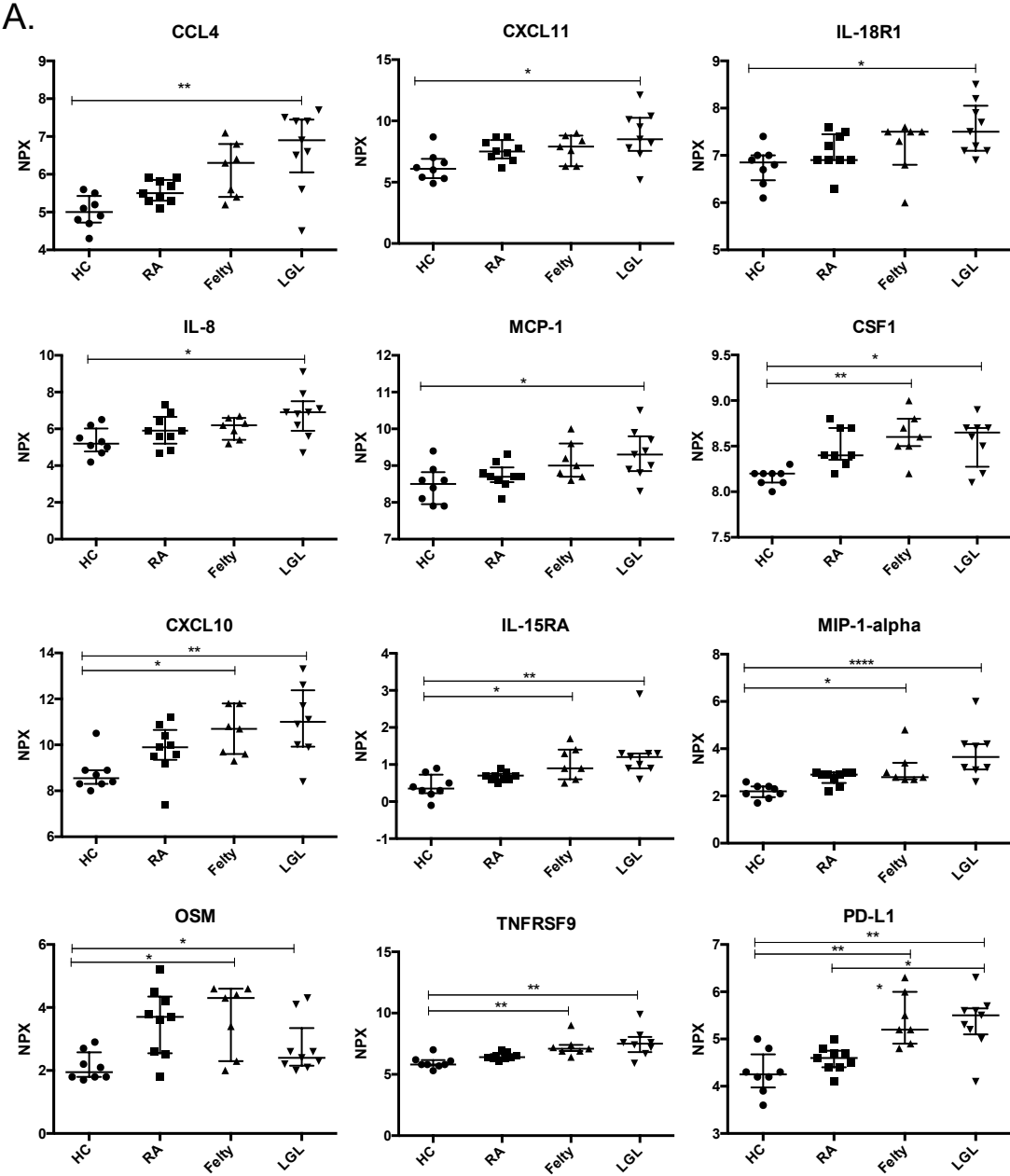


B

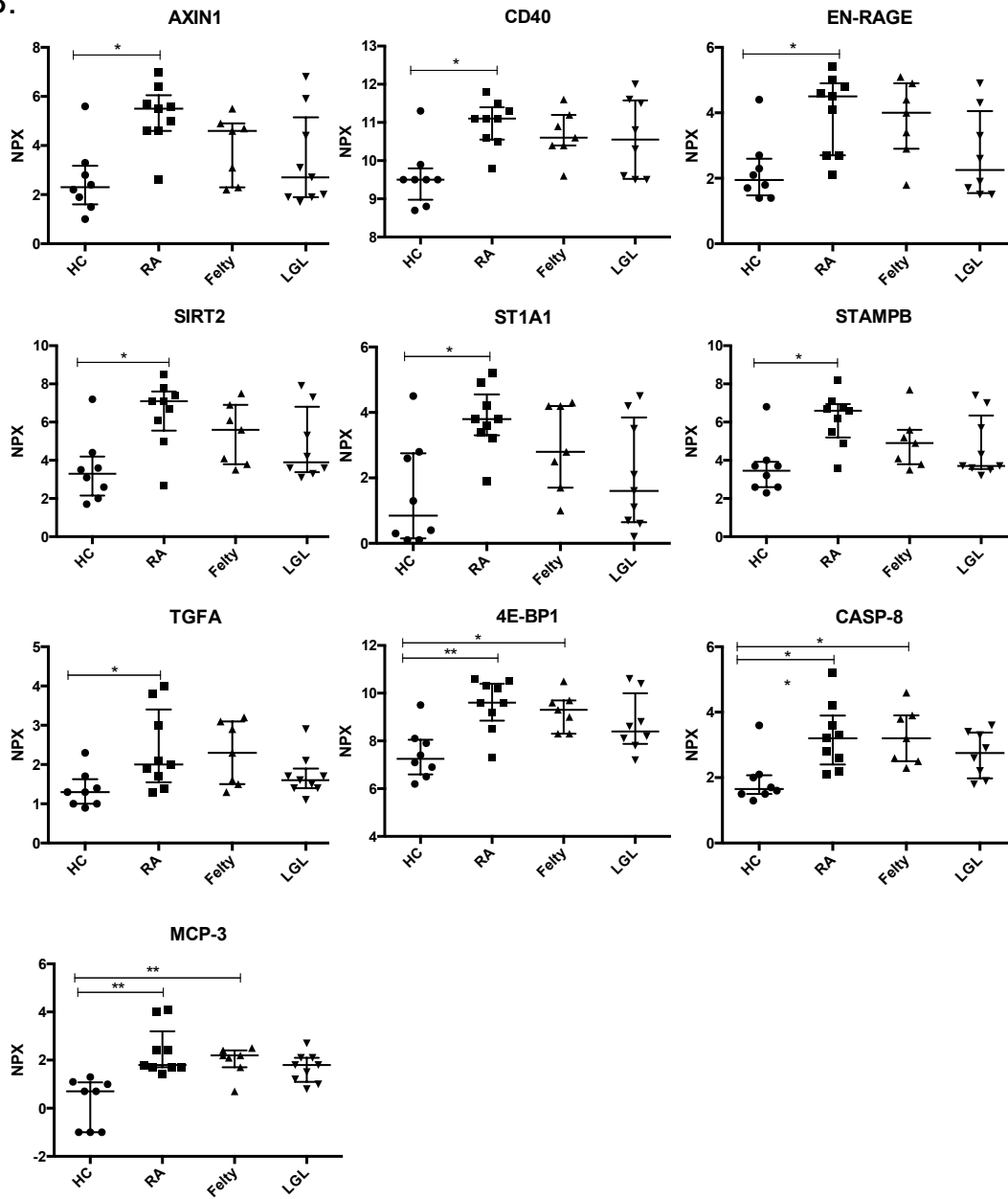


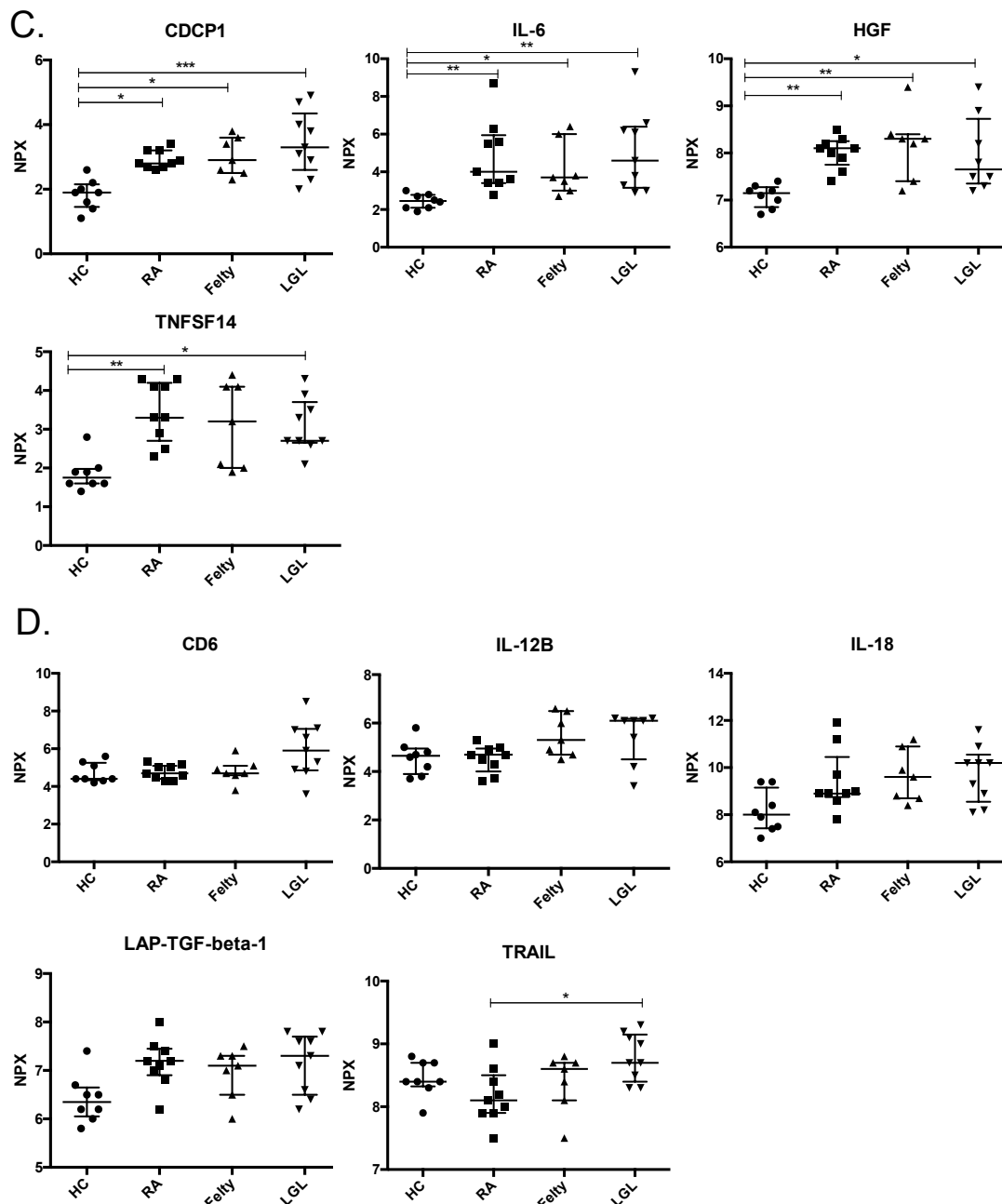
Flow cytometry results of Vβ screening showed that the largest detected CD8+ T-cell clone (Vβ22) made up 10.6% of all CD8+ T cells. The sum of all Vβ clones detected by flow cytometry made up only 38%, although the flow cytometry antibodies should cover approximately 70% of the TCR repertoire. This suggests that a clone that is not detected by the antibodies occurs in the sample. Panel A shows the results for CD8+ T cells, and panel B for CD4+ T cells.

Supplementary Figure 4. Cytokine levels in patient plasma samples.



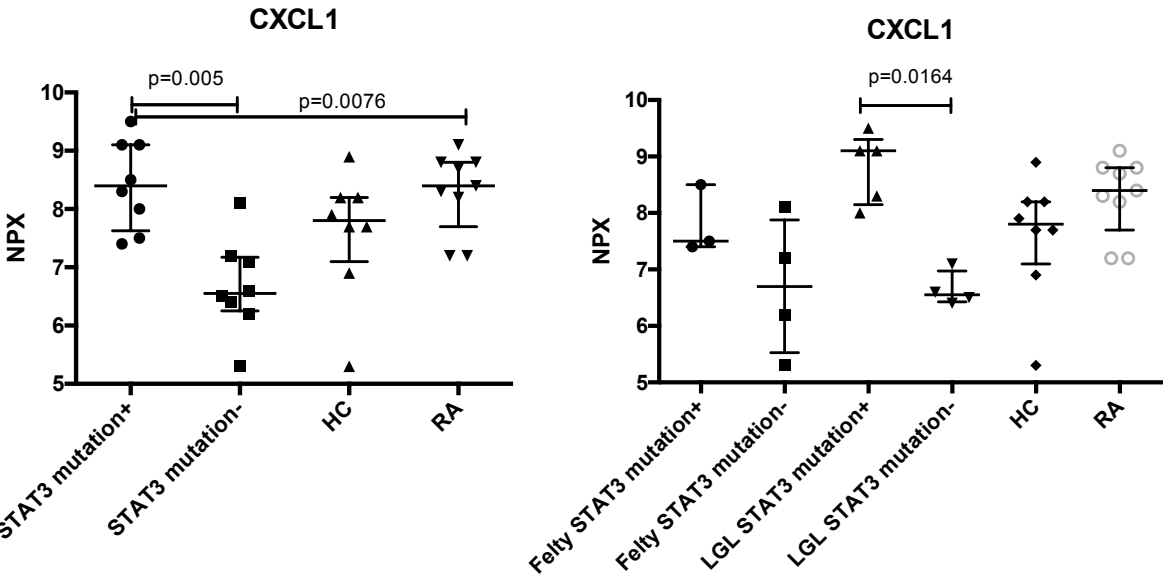
B.





Previous reports have shown that LGL leukemia patients have aberrant plasma cytokine profiles.³⁻⁹ Cytokines with a q-value <0.1 in the multiplex cytokine panel are presented in separate dotplots with the NPX (Normalized Protein eXpression, a Log₂-scale unit) - value as the y-axis. The multiplex panel included many cytokines that have been reported to be elevated in LGL leukemia, but some previously reported (sFasL, RANTES, sFas, PDGF-BB, and IL1-RA)^{4,8,9} were not included in the panel. The plots are grouped to four categories based on whether the cytokine was elevated in RA or LGL leukemia. FS patients (and other groups) are included in all analyses. A. Cytokines elevated in LGL leukemia. B. Cytokines elevated in RA patients. C. Cytokines elevated both in RA and LGL leukemia patients. D. Other cytokines; the omnibus or post-hoc tests did not show statistical difference between healthy controls and LGL/RA patients. Some cytokines were not normally distributed and had different standard deviations. Thus, the data is presented as medians and interquartile ranges in each plot. For each cytokine, a Kruskal-Wallis test was performed, followed by Dunn's multiple comparison tests as post-hoc tests. Post-hoc test p-values are presented in plots: *, $0.05 > p > 0.01$; **, $0.01 > p > 0.001$; ***, $0.001 > p > 0.0001$; ****, $p < 0.0001$.

Supplementary Figure 5. CXCL1 levels in *STAT3*-mutated vs. *STAT3*-mutation-negative patients.



Patients with *STAT3* mutations were compared with patients without *STAT3* mutations using Qlucore Omics Explorer software. The only cytokine with a q-value <0.1 in the multiplex cytokine panel was CXCL1. However, there was no statistically significant difference when compared to healthy controls. In the left panel, LGL leukemia and FS patients are grouped together based on their *STAT3* mutation status. In the right panel, FS and LGL leukemia patients were separately analyzed. In both cases, the Kruskal-Wallis test was used as an omnibus test, followed by Dunn’s multiple comparisons (adjusted p-values shown in the figure). The data is presented as medians, and the error bars show interquartile range.

References

1. Rajala HL, Olson T, Clemente MJ, et al. The analysis of clonal diversity and therapy responses using STAT3 mutations as a molecular marker in large granular lymphocytic leukemia. *Haematologica*. 2015;100(1):91-99.
2. Nikiphorou E, Sjowall C, Hannonen P, Rannio T, Sokka T. Long-term outcomes of destructive seronegative (rheumatoid) arthritis - description of four clinical cases. *BMC Musculoskelet Disord*. 2016;17:246.
3. Chen J, Petrus M, Bamford R, et al. Increased serum soluble IL-15Ralpha levels in T-cell large granular lymphocyte leukemia. *Blood*. 2012;119(1):137-143.
4. Kothapalli R, Nyland SB, Kusmartseva I, Bailey RD, McKeown TM, Loughran TP, Jr. Constitutive production of proinflammatory cytokines RANTES, MIP-1beta and IL-18 characterizes LGL leukemia. *Int J Oncol*. 2005;26(2):529-535.
5. Momose K, Makishima H, Ito T, et al. Close resemblance between chemokine receptor expression profiles of lymphoproliferative disease of granular lymphocytes and their normal counterparts in association with elevated serum concentrations of IP-10 and MIG. *Int J Hematol*. 2007;86(2):174-179.
6. Saitoh T, Matsushima T, Kaneko Y, et al. T cell large granular lymphocyte (LGL) leukemia associated with Behcet's disease: high expression of sFasL and IL-18 of CD8 LGL. *Ann Hematol*. 2008;87(7):585-586.
7. Tanaka M, Suda T, Haze K, et al. Fas ligand in human serum. *Nat Med*. 1996;2(3):317-322.
8. Liu JH, Wei S, Lamy T, et al. Blockade of Fas-dependent apoptosis by soluble Fas in LGL leukemia. *Blood*. 2002;100(4):1449-1453.
9. Zhang R, Shah MV, Yang J, et al. Network model of survival signaling in large granular lymphocyte leukemia. *Proc Natl Acad Sci U S A*. 2008;105(42):16308-16313.